Research Article | Vol. 27, No. 9 | 29 Apr 2019 | OPTICS EXPRESS 12391
Optics EXPRESS

Front propagation transition induced by diffraction in a liquid crystal light valve

ALEJANDRO J. ÁLVAREZ-SOCORRO,[1] CAMILA CASTILLO-PINTO,[1] MARCEL G. CLERC,[1] GREGORIO GONZÁLEZ-CORTES,[1] AND MARIO WILSON[2,*]

[1] *Departamento de Física and Millennium Institute for Research in Optics, FCFM, Universidad de Chile, Casilla 487–3, Santiago, Chile*
[2] *CONACYT–CICESE, Carretera Ensenada-Tijuana 3918, Zona Playitas, CP 22860, Ensenada, México*
[*] *mwilson@cicese.mx*

Abstract: Driven optical systems can exhibit coexistence of equilibrium states. Traveling waves or fronts between different states present complex spatiotemporal dynamics. We investigate the mechanisms that govern the front spread. Based on a liquid crystal light valve experiment with optical feedback, we show that the front propagation does not pursue a minimization of free energy. Depending on the free propagation length in the optical feedback loop, the front speed exhibits a supercritical transition. Theoretically, from first principles, we use a model that takes it into account, characterizing the speed transition from a plateau to a growing regime. The theoretical and experimental results show quite fair agreement.

1. Introduction

Front propagation occurs in a wide range of physical contexts such as optics, liquid crystals, granular matter, combustion, population dynamics, chemical reactions, industrial deposition processes, among others [1]. Since the seminal works of Fisher [2] and Kolmogorov, Petrovsky, and Piskunov [3] in genetics and population dynamics, respectively, on traveling fronts (called FKPP fronts) there has been an increasing interest in the study of this phenomenon. The FKPP front solutions are peculiar of connecting a stable state with an unstable one. The propagation speed of these fronts depends on the initial conditions. When the disturbance of the unstable state is bounded, the fronts always propagate with a minimal speed [1]. In liquid crystals, these fronts have been subject of intense research [4–12], since they play a fundamental role in understanding and applicating average molecular reorientations through light.

Theoretically, the interface dynamics is well understood for variational systems, i.e., systems whose dynamics is described in terms of the minimization of a physical quantity (free energy, entropy, and so forth). In contrast, nonvariational systems do not pursue a minimization of a free energy. Indeed, front propagation into an unstable state does not follow a minimization principle and its dynamics is less explored. However, front propagation between two stable states in nonvariational systems has been analyzed by Álvarez-Socorro et al [11]. The non-variationality is a generic characteristic of nonequilibrium systems [13, 14].

This work aims to investigate the effect of diffraction in the front propagation between two domains of average molecular orientations in a liquid crystal light valve (LCLV) with optical feedback. The diffraction produced by the free propagation length L governs the nonvariational effects. Based on a LCLV subjected to optical feedback experiment, front propagation into an unstable state is studied. Depending on diffraction, front speed exhibits a supercritical transition. Theoretically, using the nonlinear elasticity and optics theory, a model that accounts for this transition is inferred. The front speed exhibits a transition from a plateau to a growing regime. The theoretical and experimental results show a quite fair agreement.

#360003 https://doi.org/10.1364/OE.27.012401
© 2019 Received 12 Feb 2019; revised 14 Mar 2019; accepted 14 Mar 2019; published 17 Apr 2019

Optics EXPRESS

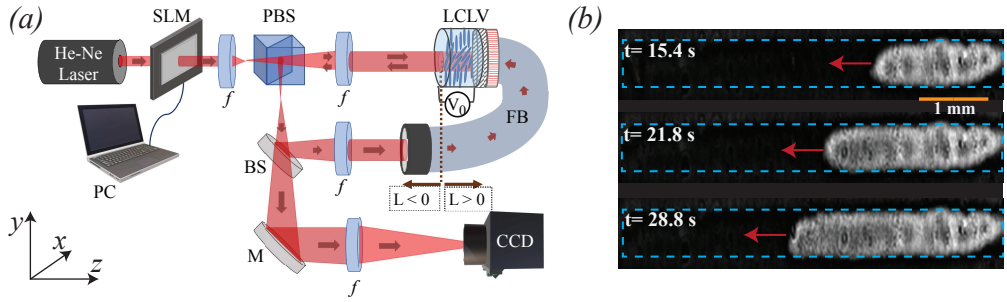

Fig. 1. Liquid crystal light valve with optical feedback. (a) Schematic representation of the experimental setup. The LCLV is composed of a nematic liquid crystal film sandwiched in between a glass and a photoconductive plate-over with a dielectric mirror. The light is injected through a He-Ne laser beam, f stands for lenses with a focal length of 25 cm, PBS represents a polarizer beam splitter, BS a beam splitter, and SLM is a spatial light modulator controlled by a computer (PC). The feedback loop is closed by an optical fiber bundle (FB). The free propagation length is denoted by L and the image in the LCLV is captured through a CCD camera. (b) Temporal snapshots sequence of the front propagation showed in the LCLV taken at $L = 0$ mm, $\nu = 1$ KHz, and $V_0 = 2.62\ V_{rms}$. Dark and light area account for different average molecular orientations, respectively. The dashed rectangles mark the illuminated region.

2. Experimental setup

A simple optical system that presents multistability and nonvariational dynamics is the LCLV with optical feedback [5–11]. Figure 1 schematically shows the used experimental setup. This setup consists in a liquid crystal cell with a photo-sensitive wall inserted in an optical feedback loop closed by an optical fiber bundle (FB). This experimental array has been designed in order to have coexisting diffraction and polarization interferences. The LCLV structure is composed by a nematic liquid crystal film between a glass with transparent electrodes (ITO) and a photoconductive plate with a deposited dielectric mirror. The liquid crystal film under consideration is a nematic LC-654, produced by NIOPIK, planar aligned, with thickness $d = 15\mu m$. It is a mixture of cyanobiphenyls, with a positive dielectric anisotropy. The optical free propagation length L drives the nonvariational effects. ITO electrodes are used to apply an external voltage V_0 across the nematic layer. The photoconductor resistance is inversely proportional to applying illumination [6].

Light suffers a phase shift while crossing the LCLV depending on the nematic director state (i.e., the average liquid crystal molecular orientation), which, in its time, modulates the effective local voltage applied to the nematic sample. Once a critical voltage is passed, the director tends to orient along the direction of the applied electric field, this reorientation changes local and dynamically, following the spatial distribution of light present in the photoconductor. Another effect of this molecular change, due to the liquid crystal birefringent nature, is an induced effective refractive index change. Thus, the LCLV can be seen as an active Kerr medium, causing a phase variation $\phi = \beta cos^2\theta = 2kd\Delta ncos^2\theta$ in the reflected beam proportional to the incoming beam intensity I_w on the photoconductive side, θ stands for the longitudinal average of the molecular reorientation [6] and $k = 2\pi/\lambda$ represents the wavenumber. An expended He-Ne laser beam, $\lambda = 633$ nm and power $I_{in} = 6.5$ mW/cm^2, linearly polarized along the vertical y axis is used as light source to illuminate the LCLV. Quasi-one-dimensional conditions are reached thanks to a computer controlled spatial light modulator (SLM) placed in the input beam. All experiments were conducted at a working temperature of 28°C. The voltage V_0 and free propagation length L are the control parameters.

Optics EXPRESS

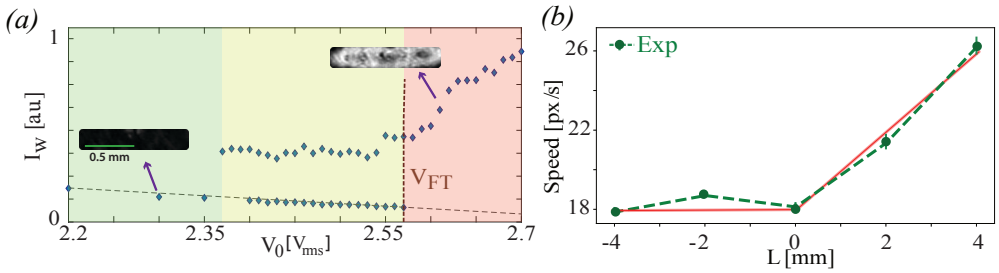

Fig. 2. Experimental characterization of the bifurcation diagram and the front propagation transition. (a) Bifurcation diagram observed in the LCLV with optical feedback constructed at $L = 0$ mm. The points account for the intensity of the reflected light by the LCLV as a function of the applied voltage V_0. The system exhibits three regions, two monostable and one bistable between the planar and reoriented state. V_{FT} accounts for the critical value of the reorientation instability, *the Fréedericksz transition*. The insets stand for respective snapshots obtained in the indicated voltages. (b) Front speed as a function of free propagation length L at $V_0 = 2.62V_{rms}$. The points account for the front speed measured in pixels per second. The dashed line is the union between consecutive experimental points. The continuous curve stands for the trend line of the experimental points.

2.1. *Experimental characterization of front propagation into an unstable state*

Thanks to the use of the spatial light modulator, a bidimensional channel is illuminated on the liquid crystal light valve of dimensions 6 mm long by 0.9 mm wide [cf. Fig. 1(b)]. By changing the voltage V_0 applied to the liquid crystal film and monitoring the evolution of light intensity that goes through the LCLV employing a CCD camera, we characterize the bifurcation diagram of the director reorientation transition. Figure 2(a) shows the bifurcation diagram obtained. For small voltage $V_0 < V_{FT}$, when the molecules are not reoriented, a little light is transmitted in the optical feedback, which corresponds to the channel being dark [see inset in Fig. 2(a)]. The critical voltage from which the molecules begin to reorient is designated by V_{FT}. On the contrary, when the director is reoriented, the transmitted light increases and then the channel turns light gray. Note that the transition of average molecular reorientation of the LCLV with optical feedback is of the first order type [4, 8]. Indeed, the transition exhibits an abrupt color change. Besides, when the voltage is varied, a hysteresis loop is observed between the average molecular configurations. The hysteresis region is between the two monostable regions.

To study the front propagation into an unstable state, we follow the strategy: initially applied voltage is small ($V_0 \ll V_{FT}$). Hence, the initial configuration is planar, and it is stable. Subsequently, the applied voltage is increased above a critical value of reorientation bifurcation ($V_0 = 2.62V_{rms} > V_{FT}$). Then the planar state becomes unstable, and the reoriented alignment is stable. The reoriented state (light color) starts to invade the planar alignment from the edges or imperfections of the channel. Figure 1(b) shows a sequence of snapshots of the observed front propagation. From the recording of the front propagation, its speed is determined. Subsequently, by changing the position of the optical fibers bundle, we can change the value of the free propagation length L, which is the distance where light diffraction occurs in our experimental setup. Figure 2(b) shows the front speed as a function of the free propagation length L at fixed applied voltage V_0. Unexpectedly, we infer that for small and negative L, the front speed is modified slightly, but for L positive this speed increases and is significantly modified. Therefore, we experimentally observe that the front speed exhibits a transition between a plateau and a growing regime. It is worthy to note that L does not change the relative stability between the director configurations, but rather changes the coupling between the molecular arrangements.

Optics EXPRESS

The origin of the front propagation transition will be elucidated in the next section.

3. Theoretical model of the LCLV with optical feedback

Based on the elastic theory, dielectric effects, and optical feedback, close to the Fréedericksz transition V_{FT}, the average molecular reorientation is given by the dimensionless model [4, 8, 11]

$$\partial_t u = \mu u + \beta u^2 + \gamma u^3 - u^5 + \partial_{xx} u + b u \partial_{xx} u + c(\partial_x u)^2, \tag{1}$$

where x and t, respectively, account for the spatial transverse coordinate and time. The order parameter $u(x,t)$ is the amplitude of the critical mode of the average molecular reorientation. μ is the bifurcation parameter, $\mu \ll 1$, that accounts for the competition between the electric and elastic force, which is proportional to $(V_0 - V_{FT})/V_{FT}$. β is a phenomenological parameter that accounts for the pretilt induced by the anchoring in the walls of the liquid crystal layer. The cubic and quintic terms stand for the competition between elastic and electrical forces induced by optical feedback [8]. The diffusion term $\partial_{xx} u$ describes the transverse elastic coupling. The coefficients b and c account, respectively, for the diffusion and the nonlinear advection. These two terms are proportional to the free propagation length L and have the same sign. Indeed, when $L = 0$, $b = c = 0$. Higher-order terms in Eq. (1) are ruled out by the scaling analysis, since $u \sim \mu^{1/4}$, $\gamma \sim \mu^{1/2}$, $\beta \sim \mu^{3/4}$, $\partial_x \sim \mu^{1/2}$, and $b \sim c \sim 0$. The previous model (1) satisfies an equation that is governed by the minimization of free energy $\mathcal{F}[u, \partial_x u]$ at $L = 0$, that is,

$$\partial_t u = -\frac{\partial \mathcal{F}}{\partial u}, \tag{2}$$

where $\mathcal{F} = \int dx[-\mu u^2/2 - \beta u^3/3 - u^4/4 + u^6/6 + (\partial_x u)^2/2]$. However, the diffraction effect generates that the diffusion and the nonlinear advection allow the emergence of permanent dynamics, such as spatiotemporal chaos [15] or oscillatory behaviors [7]. This type of behaviors is incompatible with a dynamic governed by a principle of minimization. The methodology of how to derive the parameters $\{\mu, \beta, b, c\}$ and the relation with the physical parameters are given by Clerc et al [8, 11].

The term proportional to β breaks the reflection symmetry of the amplitude u. This effect always renders the reorientation transition into a discontinuous instability with a small hysteresis. Note that positive and negative equilibria exist for $\beta, \mu > 0$. Besides, the negative values of the amplitude $u(x,t)$ has no physical sense. Figure 3 shows the bifurcation diagram of model Eq. (1). This model is characterized by exhibiting a first-order bifurcation when $\mu = 0$. Then the system presents a hysteresis region between two monostable regions. Note that this bifurcation diagram is qualitatively similar to that observed experimentally [cf. Fig. 2(a)].

An ideal region to study fronts into an unstable state is $\mu > 0$. In this region of parameter space, there are fronts between the planar unstable u_p and stable reoriented state u_+. Figure 4 shows the front propagation for $\mu > 0$. In order to study the effects of nonvariational terms, we consider a front solution initially with $b = c = 0$ and at a given time ($t = 20$) we activate the nonvariational effects ($b = 0$ and $c = -30$). In the variational regime, the minimal front speed v_{min} is determined by the linear terms, *marginal criterion* [1], which has the explicit expression $v_{min} = 2\sqrt{\mu}$. Indeed, if the values of the nonlinear parameters are changed, the front speed does not change. From Fig. 4, we infer that when the nonvariational terms are included the profile of the front is modified. The front solution exhibited a readjust of the spatial profile where the front suffers a back propagation, and after this readjust, the front solution acquires a form with which it spreads with the marginal speed. Figure 4 depicts the front profiles without and with the influence of non-variational terms. Unexpectedly, although the front profile is markedly modified, the front speed remains constant.

To analyze how the front speed is modified as a function of the non-variational terms, we have numerically measured the front speed as a function of $b = c = L$. This is consistent with

Optics EXPRESS

the functional dependence of the parameters as a function of the free propagation length L. Figure 3(b) summarizes the front speed as a function of the free propagation length L. We observe that for free negative propagation lengths the front speed is constant and as it increases the numerical precision it tends to the front speed predicted by the marginal criterion [see Fig. 3(b)]. It is well-known that numerical discretization effects modify this speed [12]. For free positive propagation lengths, we observed that the speed of the front grows linearly with L. Hence, we observe that the front speed presents a transition between a plateau and a growing regime, which is consistent with experimental observations [cf. Figs. 2(b) and 3(b)]. Indeed, the system exhibits a transition between fronts where its speed is determined by the marginal criterion (pulled front [1]) to fronts where the nonlinear terms determine the speed, nonlinear criterion (pushed front [1]). A pulled-pushed transition of fronts, with a speed transition diagram similar to that shown in Fig. 3(b), is well-known in a cubic reaction-diffusion model when the nonlinear terms are modified [16]. To figure out how the front speed is modified by the presence of the nonvariational terms a perturbative analysis can be performed.

4. Analytical and numerical analysis of the front speed

Due to the transition between pulled-pushed fronts occurs at free propagation length $L = 0$, we can consider the nonlinear diffusion and advection terms as perturbatives ($b, c \ll 1$). Let us consider $u_f(x - v_0 t)$ as the front solution for the unperturbed problem of Eq. (1) with $b = c = 0$, where $v_0 \geqslant 2\sqrt{\mu}$ is the front speed. To calculate the front speed for the perturbed problem, we consider the following ansatz,

$$u(x,t) = u_f\left(z \equiv x - v_0 t - \dot{P}(t)\right) + w(x - v_0 t - p(t)), \tag{3}$$

where z is the coordinate in co-moving system, $\dot{P}$ and w account for the correction of the front speed and the profile function, respectively. Moreover, $\dot{P}$ and w are of order of $b \sim c \sim \epsilon$, where $\epsilon \ll 1$ is a small control parameter. Introducing the ansatz (3) in Eq. (1) and leaving only the

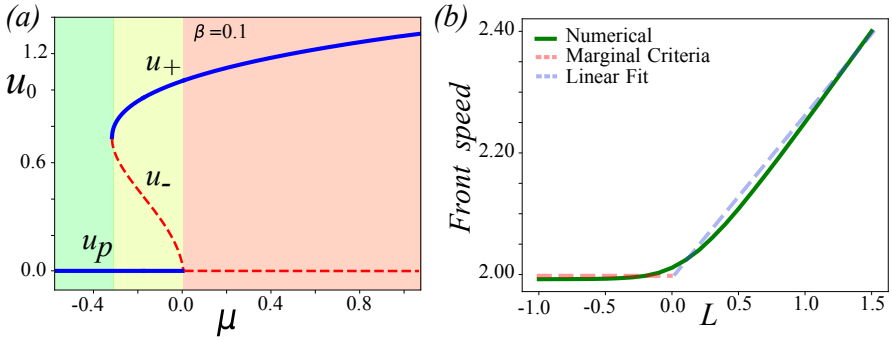

Fig. 3. Characterization of bifurcation diagram and front speed of model Eq. (1). (a) Bifurcation diagram of Eq. (1). Equilibrium amplitude u_o as a function of the parameter μ for fixed β. The continuous and dashed curves account for stable and unstable equilibrium, respectively. These curves were obtained by solving the algebraic equation $0 = \mu u_0 + \beta u_0^2 + u_0^3 - u_0^5$; u_p, u_-, and u_p account for the upper, middle, and lower equilibrium branch, respectively. The system exhibits three regions, two monostable and one bistable. (b) Front speed as a function of free propagation length L. The continuous curve shows the front speed of model Eq. (1) obtained numerically with $\mu = 1.0$, $\beta = 0.1$, and $b = c = L$. The dashed horizontal curve accounts for the minimal front speed using the marginal criterion $v_{min} = 2\sqrt{\mu}$.

Optics EXPRESS

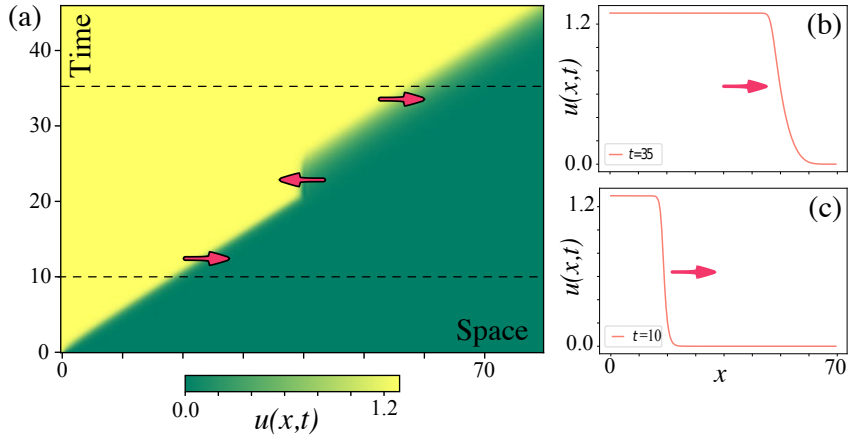

Fig. 4. Front propagation into an unstable state of model Eq. (1). (a) Spatiotemporal evolution of amplitud of critical model $u(x,t)$ of model Eq. (1) by $\mu = 1.0$, $\beta = 0.1$, and $b = 0$. Temporal evolution of the front propagation after ($c = 0$, $t < 20$) and before ($c = -30$, $t \geqslant 20$) consider the nonvariational advection term. The arrows show the direction of front propagation in the respective periods. Front profiles at $t = 35$ (b) and $t = 10$ (c), respectively.

terms up to ϵ order, after straightforward calculations, we get the linear equation

$$\mathcal{L}w = -\dot{p}(t)\partial_z u_f - b u_f \partial_{zz} u_f - c(\partial_z u_f)^2, \tag{4}$$

where the linear operator has the form $\mathcal{L} \equiv [\mu + 2\beta u_f + 3u_f^2 - 5u_f^4 + v\partial_z + \partial_{zz} + b(u_f\partial_{zz} + \partial_{zz}u_f) + 2c\partial_z u_f \partial_z]$. To solve this linear equation, we use the Fredholm alternative or solvability condition [17] and obtain

$$\dot{p}(t) = v_{nv} \equiv -b\frac{\langle\phi|\, u_f\partial_{zz}u_f\rangle}{\langle\phi|\,\partial_z u_f\rangle} - c\frac{\langle\phi|\,(\partial_z u_f)^2\rangle}{\langle\phi|\,\partial_z u_f\rangle}, \tag{5}$$

where the symbol $\langle f|\, g\rangle \equiv \int_{-\infty}^{\infty} f(z)g(z)dz$ and the function $\phi(z)$ belong to the kernel of the adjoint operator of $\mathcal{L}$, which is independent of diffraction effect. The ϕ function is only accessible numerically. As a matter of fact, the correction of the front speed of nonvariational origin is proportional to the free propagation length L. When $L > 0$ (L<0), the previous integrals are negative (positive) then v_{nv} is positive (negative). Hence the front speed has two contributions, one of variational origin given by the linear criterion and another nonlinear one given by the nonvariational effects, i.e.,

$$v = v_0 + v_{nv}. \tag{6}$$

Therefore, from this perturbative analysis, it is expected that the front speed increases or decreases with the free propagation length L. However, numerically only for positive diffraction, the front speed increases linearly with the free propagation length [cf. Fig. 3(b)]. Figure 5 shows how the speed and the profile of the front are modified when the free propagation length L is changed. Therefore, for $L > 0$, the system exhibits an excellent qualitative agreement with Eq. (5). Despite the above calculation, for $L < 0$, the speed of the front remains at the minimum speed in contradiction with Eq. (6). This behavior can be understood in the following way, the front modifies its asymptotic profile (cf. Figs. 4 and 5), which increases its propagation speed given by the linear criterion [18], so that it cancels the speed decrement induced by the nonvariational effects. Then, the previous perturbative analysis cannot be valid because the base

Optics EXPRESS

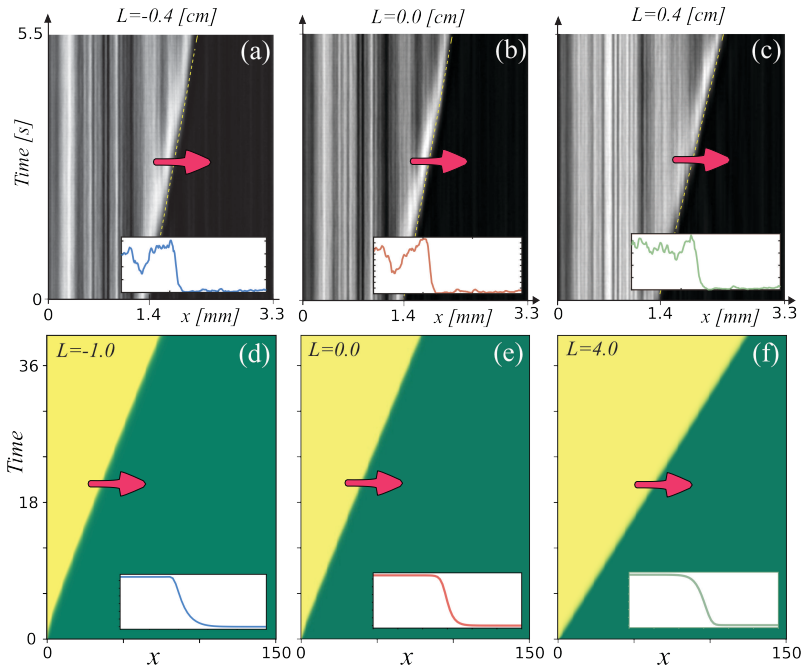

Fig. 5. Spatiotemporal propagation of front solution into an unstable state for different free propagation lengths. Top panels account for front propagation in the experiment by $L = -0.4$ cm (a), $L = 0.0$ cm (b), and $L = 0.4$ cm (c), respectively. Bottom panels stand for the front propagation of model Eq. (1) by $\mu = 1.0$, $\beta = 0.1$, and free propagation length $L = -1.0$ (d), $L = 0$ (e), and $L = 4.0$ (f). The insets account for the front profile at a given instant experimentally and numerically, respectively.

solution is modified and it is not a small correction. This mechanism explains the origin of the pull-pushed transition of fronts, when the disturbance tries to decrease the fronts speed, it adapts their shape to maintain the minimum speed. Also, when the disturbance increases the speed of propagation, the system responds by increasing the speed. Therefore, the system exhibits a pull-pushed transition of fronts at zero free propagation length in the optical feedback loop, $L = 0$, when the disturbance begins to increase the minimum speed. Spatiotemporal diagrams are an adequate tool to characterize this type of transitions. When the parameters are modified, if the speed remains unchanged, pulled fronts will not produce any noticeable change in the spatiotemporal diagram, however when fronts are pushed, the spatiotemporal diagram presents a change in the front position slope (cf. Fig. 5).

5. Conclusions and remarks

Based on a liquid crystal light valve experiment with optical feedback, we have investigated a mechanism of speed control in interfaces connecting a stable with an unstable state based on varying the free propagation length, showing a supercritical transition from a plateau speed to an increasing speed regime, *pulled-pushed front transition*. Experimental and theoretically, we have characterized this supercritical transition, which result shows quite fair agreement.

The possibility of having different molecular domains with varying effective refractive indices, being able to manipulate the speed between these domains, allows the opportunity of having switches between electronic and optical elements. The presented results open the possibility of

Optics EXPRESS

novel photonic devices in such direction.

Funding

Comisión Nacional de Investigación Científica y Tecnológica (2015-21151618, 2017-21171672); Fondo Nacional de Desarrollo Científico y Tecnológico (1180903).

Acknowledgments

A. J. Álvarez-Socorro, C. Castillo, M. G. Clerc and G. González-Cortés gratefully acknowledge the financial support from the Millennium Institute for Research in Optics (MIRO).

References

1. W. van Saarloos, "Front propagation into unstable states," Phys. Reports **386**(2), 29–222 (2003).
2. R. A. Fisher, "The wave of advance of advantageous genes," Ann. Eugen. **7**, 353–369 (1937).
3. A. N. Kolmogorov, I. G. Petrovskii, and N. S. Piskunov, "A study of the diffusion equation with increase in the amount of substance, and its application to a biological problem," Bull. Mosc. Univ. Math. Mech. **1**(6), 1–26 (1937). Reprinted in: V. M. Tikhomirov (ed.), *Selected Works of A. N. Kolmogorov, vol. 1* (Kluwer, 1991). Also in: O. A. Oleinik, *I. G. Petrowsky Selected Works, Part II* (Gordon and Breach, 1996).
4. M. G. Clerc, S. Residori, and C. S Riera, "First-order Fréedericksz transition in the presence of light-driven feedback in nematic liquid crystals," Phys. Rev. E **63**, 060701 (2001).
5. S. Residori, A. Petrossian, T. Nagaya, C. S. Riera, and M. G. Clerc, "Fronts and localized structures in a liquid crystal-light-valve with optical feedback," Phys. D: Nonlinear Phenom. **199**, 149–165 (2004).
6. S. Residori, "Patterns, fronts and structures in a liquid crystal-Light-Valve with optical feedback," Phys. Reports **416**, 201–272 (2005).
7. M. G. Clerc, A. Petrossian, and S. Residori, "Bouncing localized structures in a liquid crystal light-valve experiment," Phys. Rev. E **71**, 015205 (2005).
8. M. G. Clerc, T. Nagaya, A. Petrossian, S. Residori, and C. S. Riera, "First-order Frédericksz transition and front propagation in a liquid crystal light valve with feedback," Euro Phys. J. D **28**(3), 435–445 (2004).
9. F. Haudin, R. G. Elias, R. G. Rojas, U. Bortolozzo, M. G. Clerc, and S. Residori, "Driven Front Propagation in 1D Spatially Periodic Media," Phys. Rev. Lett. **103**, 128003 (2009).
10. F. Haudin, R. G. Elias, R. G. Rojas, U. Bortolozzo, M. G. Clerc, and S. Residori, "Front dynamics and pinning-depinning phenomenon in spatially periodic media," Phys. Rev. E **81**, 056203 (2010).
11. A. J. Álvarez-Socorro, M. G. Clerc, G. González-Cortés, and M. Wilson, "Nonvariational mechanism of front propagation: Theory and experiments," Phys. Rev. E **95**, 010202 (2017).
12. K. Alfaro-Bittner, M. G. Clerc, M. García-Nustes, and R. G. Rojas, "π-kink propagation in the damped Frenkel-Kontorova model," Europhys. Lett. **119**(4), 40003 (2018).
13. I. Prigogine and G. Nicolis, *Self-Organization in Non-Equilibrium Systems,* (John Wiley & Sons Inc., 1997).
14. H. Haken, *Advanced synergetics: Instability hierarchies of self-organizing systems and devices,* (Springer Verlag, 1983).
15. M. G. Clerc, G. González-Cortés, V. Odent, and M. Wilson, "Optical textures: characterizing spatiotemporal chaos," Opt. Express **24**(14), 15478–15485 (2016).
16. K. P. Hadeler and F. Rothe, "Travelling fronts in nonlinear diffusion equations," J. Math. Biol. **2**(3), 251–263 (1975).
17. E. I. Fredholm, "Sur une classe d'equations fonctionnelles," Acta Math. **27**, 365-390 (1903).
18. D. Mollison, "Spatial contact models for ecological and epidemic spread," J. R. Statist. Soc. B **39**, 283-326 (1977).